CONF-9108150--5

58906-00-105

December 1991

# A TWO-DIMENSIONAL ACAR STUDY OF UNTWINNED $YBa_2Cu_3O_{7-x}$*

ANL/CP--75104

DE92 007383

L.C. Smedskjaer

*Materials Science Division*
*Argonne National Laboratory, Argonne, IL 60439*

and

A. Bansil

*Physics Department*
*Northeastern University, Boston, MA 02115*



jmc

## DISCLAIMER



**Invited presentation for Proceedings of 9th International Positron Annihilation Conference, Hungary, 1991.**

*Work supported by the U.S. Department of Energy, BES-Materials Sciences under contract #W-31-109-ENG-38.

Keywords: Hi-$T_c$ super conductors, Fermi Surfaces, $YBa_2Cu_3O_{7-x}$

# A Two-Dimensional ACAR Study of Untwinned $YBa_2Cu_3O_{7-x}$

L.C. Smedskjaer[1] and A. Bansil[2].

[1] Materials Science Division, Argonne National Laboratory, Argonne, IL 60439.

[2] Physics Department, Northeastern University, Boston, Massachusetts 02115

## ABSTRACT

We have carried out 2D-ACAR measurements on an untwinned single crystal of $YBa_2Cu_3O_{7-x}$ as a function of temperature, for five temperatures ranging from 30K to 300K. We show that these temperature dependent 2D-ACAR spectra can be described to a good approximation as a superposition of two temperature *independent* spectra with temperature dependent weighting factors. We show further how the data can be used to correct for the 'background' in the experimental spectrum. Such a 'background corrected' spectrum is in remarkable accord with the corresponding band theory predictions, and displays in particular clear signatures of the electron ridge Fermi surface.



*To appear Proc. of the 9'th Int. Positron Annihilation Conf. Hungary (1991)*
*(Invited talk.)*

Keywords: Hi-$T_c$ super conductors, Fermi Surfaces, $YBa_2Cu_3O_{7-x}$

# A Two-Dimensional ACAR Study of Untwinned $YBa_2Cu_3O_{7-x}$

L.C. Smedskjaer[1] and A. Bansil[2].

[1] Materials Science Division, Argonne National Laboratory, Argonne, IL 60439.

[2] Physics Department, Northeastern University, Boston, Massachusetts 02115

## ABSTRACT

We have carried out 2D-ACAR measurements on an untwinned single crystal of $YBa_2Cu_3O_{7-x}$ as a function of temperature, for five temperatures ranging from 30K to 300K. We show that these temperature dependent 2D-ACAR spectra can be described to a good approximation as a superposition of two temperature *independent* spectra with temperature dependent weighting factors. We show further how the data can be used to correct for the 'background' in the experimental spectrum. Such a 'background corrected' spectrum is in remarkable accord with the corresponding band theory predictions, and displays in particular clear signatures of the electron ridge Fermi surface.

## INTRODUCTION

Positron annihilation (2D-ACAR) studies of $YBa_2Cu_3O_{7-x}$ started immediately after the discovery of this archetypal high temperature superconductor. The 2D-ACAR experiment is ideally suited to answer one of the fundamental questions that arose early in the game, namely, does the electron momentum density in the new materials possess Fermi surface breaks like the conventional metals or does it not. The experimental results in this regard would provide guidance in searching for a suitable theoretical description of the electronic structure, and thus help in developing an understanding of the mechanism responsible for the occurrence of high superconducting transition temperatures. More generally, the accuracy of any specific electronic structure model can in principle be assessed by comparing the predicted 2D-ACAR spectra with the corresponding observations, although such comparisons to date have been possible only for the local density (LDA) based band theory model, which is the only model where detailed theoretical predictions are currently available.

It is appropriate to make a few brief comments concerning two other commonly used techniques for exploring the electronic structure and Fermiology of materials, i.e. dHvA and angle-resolved photoemission (ARPES). Compared to dHvA, the 2D-ACAR experiment possesses the advantage of

not requiring long mean free paths. Also, since positron annihilation probes the bulk electronic structure, the technique does not suffer from the surface sensitivity of the ARPES. On the other hand, the annihilation process involves all occupied electron states, and therefore the amplitude of the spectral features associated with, for example the Fermi surface, is typically only a few percent of the total 2D-ACAR signal. In contrast, dHvA and ARPES involve selective excitation of a small number of electronic states in the vicinity of the Fermi energy. Bearing these considerations in mind, it makes sense to view dHvA, ARPES, and 2D-ACAR as complementary techniques, and indeed, the most convincing recent evidence for the existence of a Fermi surface in $YBa_2Cu_3O_7$ in essential accord with the band theory predictions has been pieced together by combining the results of these three spectroscopies.

The early positron studies of $YBa_2Cu_3O_{7-x}$ all involved *twinned* specimens. The first 2D-ACAR results were reported by the Geneva group for projections in the a-b plane [1], and from Argonne for the c-projection [2], the latter projection has since been used in most studies due to its suitability in investigating the Fermiology of layered compounds. The initial interpretation of these 2D-ACAR data in terms of the existence of the Fermi surfaces, gave way to a period of lull in the field as subsequent experiments failed to convincingly confirm these conclusions, and thus a consensus concerning a Fermi surface interpretation of the 2D-ACAR data did not emerge in the positron community [3,4]. A comprehensive overview of the work on twinned samples has been given by Barbiellini et al [5].

A new chapter in positron studies of superconductors was opened recently when *untwinned* $YBa_2Cu_3O_{7-x}$ specimens were employed. The first announcement of the untwinned 2D-ACAR results was made by the Texas-Livermore effort [6], followed immediately afterwards by the Argonne-Northeastern effort [7]. Most important, the data from these two independent experiments are very similar, and further both groups make a very similar interpretation in terms of the existence of Fermi surfaces in this material. The preliminary results of experiments in Geneva on an untwinned $YBa_2Cu_3O_{7-x}$ single crystal have also been reported at this meeting [8], and appear to be consistent with the aforementioned measurements. It is clear that the coming on line of the untwinned specimens marks a significant milestone, and that the application of the 2D-ACAR technique in exploring the Fermiology of the high-$T_c$'s can now go forward with a degree of confidence.

The crucial role of theoretical model computations in the preceding developments deserves mention. The importance of calculations in interpreting 2D-ACAR spectra, even in simple materials, was recognized rather early in the field [9]. Such theoretical predictions take on an added significance in the high-$T_c$'s due to the complexity of their crystal structures. Following the first 2D-ACAR computations of Bansil et al [10-13] in $YBa_2Cu_3O_7$ within the band theory framework, a number of groups have reported similar theoretical results [5,14-17]; the important point which bears emphasis is that the results from different groups are in good accord with one another, relatively smaller differences between various first principles calculations notwithstanding, and a robust picture of the band theory predictions in $YBa_2Cu_3O_7$ has emerged. These theoretical results have indeed played a crucially important role in identifying Fermi surface signatures in the 2D-ACAR spectra.

In this article, we discuss some aspects of the 2D-ACAR measurements we have recently completed on an untwinned single crystal of $YBa_2Cu_3O_{7-x}$ as a function of temperature. The data were collected at five temperatures ranging from 30K to 300K, and thus include the superconducting as well as the normal metallic state. In analyzing the temperature dependent spectra using matrix manipulation techniques, we find that the data can be described quite well as a superposition of two temperature independent spectra with temperature dependent relative weights. We outline our method of analysis, and the implications of our results for understanding 2D-ACAR spectra in $YBa_2Cu_3O_{7-x}$. Most important, we show the temperature dependent data can be exploited to obtain from the measurements what may be considered a 'background corrected' 2D-ACAR spectrum, which is shown to be in remarkable agreement with the corresponding band-theory predictions. The question of comparing theory and experiment, as well as of identifying Fermi surface signatures in the observed spectra, although considered briefly here, is mostly taken up in the article by Bansil and Smedskjaer [18].

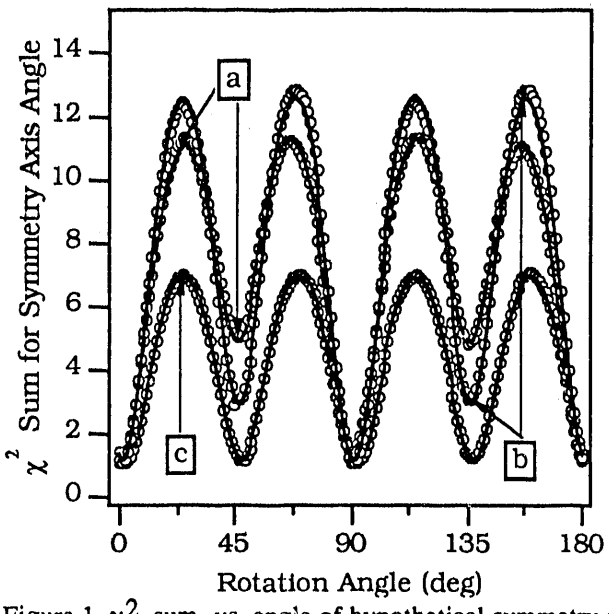


Figure 1. $\chi^2$ sum vs. angle of hypothetical symmetry axis a: untwinned 300K, b: untwinned 30K, c: twinned 30K. Solid curves are harmonic fit to the data.

## RESULTS AND DISCUSSION

We have obtained 2D-ACAR data in the c-axis projection for *untwinned* $YBa_2Cu_3O_{6.9}$ at 30K, 70K, 100K, 185K and 300K. The total number of counts were 100 Mcounts for the 30K and 300K spectra and 16-22 Mcounts for the remaining spectra. The resolution (FWHM) due to the camera and the sample size is 0.4-0.5 mrad. At low temperatures this will be the effective resolution, while the thermal velocity of the positron gives rise to resolution broadening at higher temperatures. Assuming an effective positron mass of one, the overall resolution at 300K is 0.7 mrad.

The sample was an *untwinned* single crystal of $YBa_2Cu_3O_{6.9}$ (0.9 x 1.6 x 0.1 $mm^3$) with a transition temperature of 91K and a transition width of 1K. The sample was supported by a 25 μm dia. tungsten wire. Based upon separate experiments we estimate the background contribution from the sample support to be 5-10% of the annihilations. The crystal c-axis was oriented *in situ*, while the precise a (b) axis orientation was deduced from the data as described below.

For each spectrum the coincidence field and the floodfields used for the efficiency correction were collected intermittently in order to reduce the effects of possible instrumental instabilities. All data were collected in listmode allowing for a dispersion of 11 μrad/channel in momentum space. After verifying that the data displayed $C_{2v}$ symmetry, they were subsequently symmetrized to augment the signal to noise ratio [19].

The spectral symmetries were studied in a manner similar to that of Ref.[19], i.e. by calculating the Chi-square sum for the hypothesis that the symmetry axis makes a given angle, $\phi$, with the instrumental $p_x$ axis. Typical results are shown in Fig. 1 for a twinned as well as an untwinned sample. The minima for the twinned sample are all around 1, and one concludes that these data possess $C_{4v}$ symmetry. In contrast it is seen that the minima at 45 (135) degrees for the untwinned sample are significantly larger than 1, while the minima at 90 (180) degrees are 1. Thus the untwinned sample only possesses $C_{2v}$ symmetry. It is also seen from Fig. 1 that the minima do not coincide exactly with 45, 90, 135 and 180 degrees. This is due to a slight misalignment of the sample a (b) axis relative to the instrument axis. By an analysis of Fig.1 in terms of harmonics one can determine the extent of the misalignment and correct the data accordingly.

The import of Fig. 1 is twofold; firstly, one notes that the symmetry properties for the present *untwinned* data are satisfying. Secondly, one notes that the symmetry properties depend upon temperature. This is more clearly illustrated in Fig. 2, where the relative intensity of the 90 deg. periodic harmonic is plotted as a

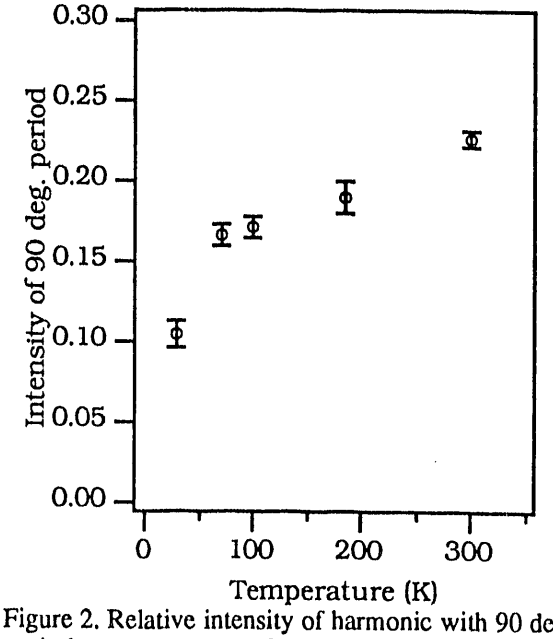


Figure 2. Relative intensity of harmonic with 90 deg. period vs.temperature for the untwinned sample. Errors are given conservatively.

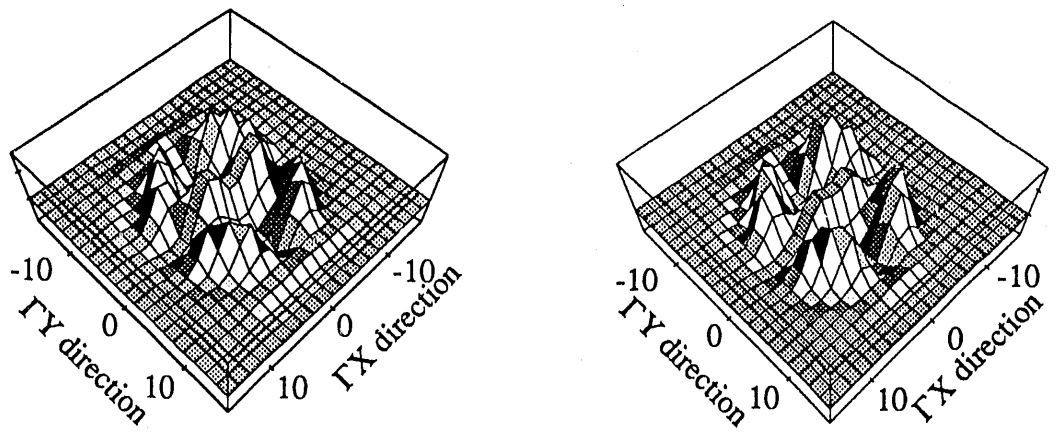


Figure 3. Anisotropic part of 2D-ACAR data for the untwinned sample. Left: 300K, right: 30K. The pixel size is 1.57 by 1.57 mrad, which is about twice the resolution (FWHM) at 300K.

function of temperature. For an ideally *twinned* sample this harmonic would be identically zero; the maximum value is 1.0. It is seen that the intensity roughly doubles between 30K and 300K.

In Fig. 3 the anisotropic parts of the spectra, obtained by subtracting smooth isotropic functions from the observed data, are shown for the untwinned sample; the smooth functions used here were constrained to be less than the measured spectrum at all momenta. (Spectra obtained at intermediate temperatures fall in between the results shown in Fig. 3, and are not shown.) It is seen that the anisotropic part consists of two main features, namely a central ridge in the ΓX direction, and four mountains surrounding the ridge. In addition, a sideridge, running parallel to the ΓX direction at 13 mrad, is seen as well. In a *twinned* crystal the four mountains are present [2] ,but the central ridge takes the form of a blurred cross. It can be shown that the ridge and the sideridges possess $C_{2v}$ symmetry while the mountains are almost $C_{4v}$ symmetric. Physically, the ridge and sideridge features arise mainly from electronic states associated with the CuO chains, while the mountains can be due to both the chain states and the CuO plane states.

Fig. 4 presents sections through the spectra of Fig. 3 along the ΓY direction (i.e. perpendicular to the ridge) and shows the detailed shapes of various spectral features. The ridge and the sideridge are seen around $p_y$=0 and $p_y$=13 mrad at both temperatures. With increasing $p_x$ the sideridge becomes less prominent as it begins to overlap with the four mountains. Although the major features are similar, changes in the details of the spectral shapes are nevertheless apparent with temperature (e.g. at 300K the $p_x$ curve has a structure around 6.3 mrad, which is absent at 30K)

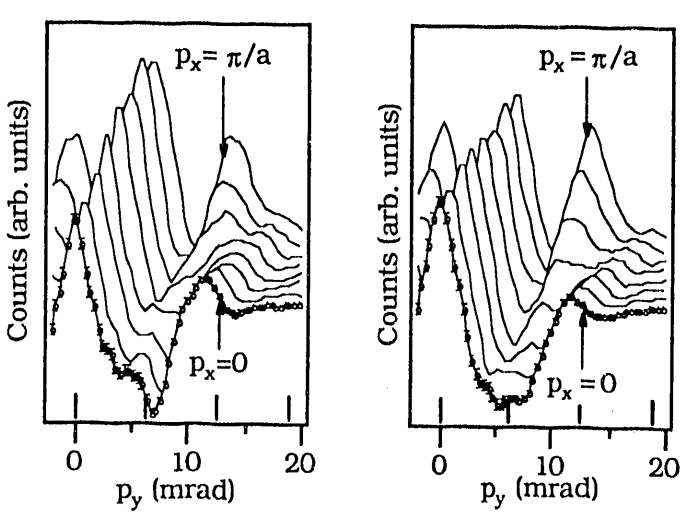


Figure 4. Sections along ΓY through spectra shown in Fig. 3. Left: 300K, right: 30K. The Γ points are indicated as vertical lines inside the frame. The dispersion is 0.39 mrad/channel .

Given their complexity, the 2D-ACAR spectra are difficult to interpret meaningfully without theoretical model

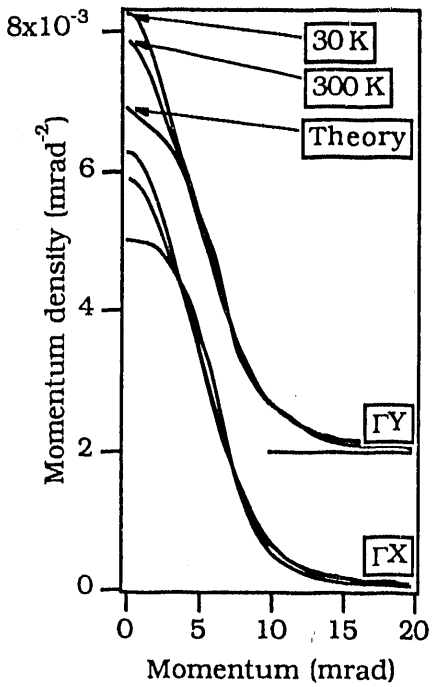


Figure 5. Comparison of two sections through the data with corresponding theoretical results.

computations, even in simpler materials. Here, we compare our measurements with the corresponding band theory based results. The relevant electron-positron momentum density in $YBa_2Cu_3O_7$ has been obtained by several groups [5,10-17]. There is a good overall accord between the results from various groups; in particular, all computations show clearly that the one-dimensional chain bands will give prominent signals in the 2D-ACAR spectra. In the present work, we compare our experimental results with the corresponding theoretical calculations of Bansil *et al* [10-13]. As previously mentioned [12] in connection with a *twinned* sample, and shown in Fig. 5 for the present *untwinned* sample, a direct comparison between the measured data and the theory leads to a discrepancy such that the experimental spectra are more peaked near the origin; Ref [12] also shows that much of this discrepancy can be removed by an isotropic background subtraction, although the origin of such a background contribution was not entirely clear. It should also be noted that similar temperature dependent discrepancies are also observed for *twinned* samples by Hoffmann *et al.* [20].

In order to understand the temperature dependent data, we first examined the possible existence of linear dependencies in the spectra. To accomplish this a new set of spectra, $\mu(\mathbf{p},T)=M(\mathbf{p},T)-\langle M(\mathbf{p})\rangle_T$, are formed by subtracting the temperature averaged spectrum $\langle M(\mathbf{p})\rangle_T$ from each of the measured spectra $M(\mathbf{p},T)$; the $\mu$ spectra (128 by 128 channels each) are organized as five column 'vectors' in a matrix $A_{m,n}$ ($m=128^2$, $n=5$). We then pose the question, whether any of the five spectra are linearly dependent on one another. With the question formulated this way, well known matrix techniques can be invoked. Specifically, we carried out the so-called singular value decomposition (SVD) [21] of the matrix A, where each column, as indicated, contains all the data points in one of the 2D-ACAR spectra. Obviously there can at most be four linearly independent $\mu$ spectra. The SVD analysis yielded four orthonormal basis vectors (denoted $U^i(\mathbf{p})$ for i=1 to 4) and each physical spectrum, $M(\mathbf{p},T)$, can then be written as a linear combination of the $U^i(\mathbf{p})$'s with associated temperature dependent coefficients $\alpha_i(T)$.

$$M(\mathbf{p},T)=\langle M(\mathbf{p})\rangle_T+\sum_{i=1}^{4}\alpha_i(T)\,U^i(\mathbf{p}) \qquad (1)$$

Inspection showed that one of the coefficients dominated and had a 5 times larger temperature dependence than the remaining coefficients. We thus arrive at the approximate representation:

$$M(\mathbf{p},T)\approx\langle M(\mathbf{p})\rangle_T+\alpha_1(T)\,U^1(\mathbf{p}) \qquad (2)$$

where $\alpha_1(T)$ denotes the coefficient with the largest variation. The most important implication of equation 2 is that the data can be expressed to a good approximation as a weighted average of *two* temperature independent spectra.Therefore, equation (2) may be cast in the equivalent form:

$$M(\mathbf{p},T) = F(\mathbf{p}) + I(T)\,(B(\mathbf{p})-F(\mathbf{p})) \qquad (3a)$$
$$= (1-I(T))\,F(\mathbf{p}) + I(T)\,B(\mathbf{p}) \qquad (3b)$$

where we have formally replaced the spectra $\langle M(\mathbf{p})\rangle_T$ and $U^1(\mathbf{p})$ occurring in equation (2) by two other spectra $F(\mathbf{p})$ and $B(\mathbf{p})$. The motivation for so recasting equation (2) is that form 3(b) is often

invoked in positron defect spectroscopy in connection with annihilation spectrum from a sample with a single species of defects, with F(**p**) and B(**p**) corresponding to the spectra from the perfect bulk material and the defects respectively, and I(T) to the trapping probability. The fact that the present spectra admit a representation of form (3) implies that our temperature dependent data may be viewed as a superposition of two types of annihilations. It makes sense to consider one of these as the bulk annihilations, F(**p**), and the remainder as 'background' annihilations, B(**p**). We emphasize that the physical origin of such a background is unclear, although in analogy with the defect spectroscopy, it will be consistent to interpret the background to be the result of shallow traps; such a mechanism has previously been invoked in connection with simple metals (see e.g. [22]).

In defect spectroscopy (see e.g.[23]), the spectra corresponding to F(**p**) and B(**p**) can be determined from direct observations in the limiting situations, i.e, at high temperatures there may be no trapping so that I(T)=0, and at low temperatures there may be complete trapping which implies I(T)=1. There is no indication that in the present case any of the spectra represent such limiting cases, leaving the forms of the spectra F(**p**) and B(**p**) experimentally undetermined. Despite this, we show below that progress is possible in assessing the extent to which the experimental results are consistent with the theoretically predicted 2D-ACAR spectrum T(**p**) for bulk annihilation.

To this end, note that by writing an equation of form 3(b) at two different temperatures $T_1$ and $T_2$, we may formally eliminate the term B(**p**), and thus express F(**p**) as a linear combination of any two measured spectra $M(\mathbf{p},T_1)$ and $M(\mathbf{p},T_2)$, i.e.

$$F(\mathbf{p}) = (1-\beta)\, M(\mathbf{p},T_1) + \beta\, M(\mathbf{p},T_2) \qquad (4)$$

where $\beta$ is easily obtained in terms of $I(T_1)$ and $I(T_2)$. We now argue that we may make an absolute comparison between theory and experiment by *fitting* the constant $\beta$ on the right side of (4) to the band theory predicted 2D-ACAR, T(**p**). However, since T(**p**) has not been normalized an additional overall normalization factor, $\gamma$, must be introduced as well. Denoting the fitted values by $\tilde{\beta}$ and $\tilde{\gamma}$, we thus obtain the distribution

$$H(\mathbf{p}) = \tilde{\gamma}\,((1-\tilde{\beta})\, M(\mathbf{p},T_1) + \tilde{\beta}\, M(\mathbf{p},T_2)) \qquad (5)$$

where the constant $\tilde{\gamma}$ is an overall normalization factor, and $\tilde{\beta}$ is the important factor which determines the shape of the spectrum. H(**p**) can be considered a 'background corrected' experimental spectrum. The specific values of $\tilde{\beta}$ and $\tilde{\gamma}$ were determined by using only the ΓY theoretical and experimental sections (the results if another direction is used in the fitting procedure instead are similar). We obtain however a good fit between theory and experiment not only along ΓY but in other directions as well. In order to obtain the best statistical accuracy, the 30K and 300K pair of spectra were used to obtain the constants $\tilde{\beta}$ and $\tilde{\gamma}$.

The result is shown in Fig. 6, which when compared to Fig. 5, shows the dramatic improvement in the fit between theory and the 'background corrected' experimental data H(**p**) along all directions. It is especially noted that the strong anisotropy between the ΓX and ΓY directions, predicted by theory, is now also seen experimentally; this anisotropy is less clear in Fig. 5. Regarding the background spectrum B(**p**), it is unfortunate that it must be left undetermined at present; information obtained

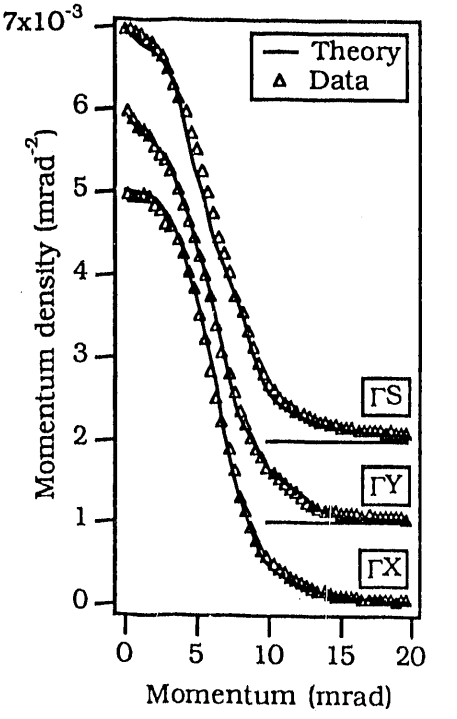


Figure 6. Comparison between theory and the the 'background corrected' experimental data H(p).

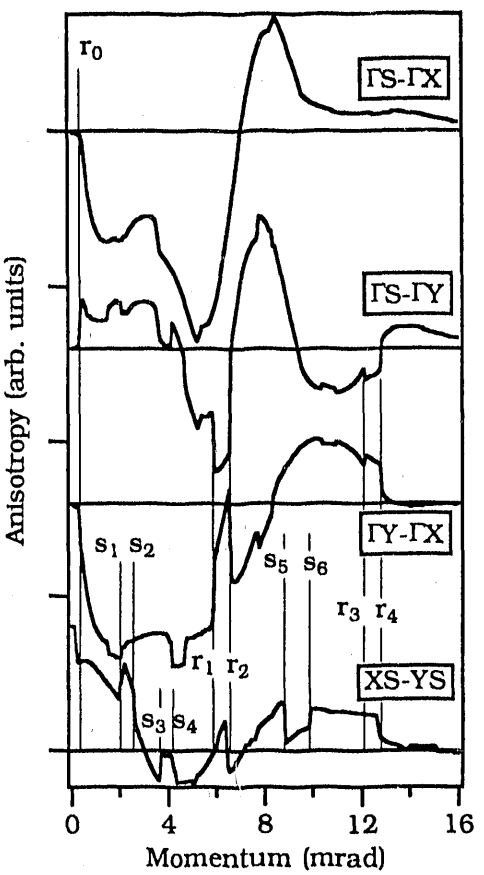


Figure 7. Theoretical difference sections in $YBa_2Cu_3O_7$. Vertical lines mark positions of various Fermi surface features denoted by $r_0$, $s_1$, etc. (see text).

independently of the present data will be needed to determine B(**p**).

A finer level of comparison between theory and experiment may be made by considering anisotropies in the spectra in the form of differences in the distribution along various pairs of directions. In this connection, it is helpful first to consider Fig. 7 which displays a representative set of theoretical difference sections [11,12]. As expected, the structure in the spectra is now more apparent than in the original theoretical distributions of Figs. 5 and 6. The complicated nature of the curves in Fig. 7 reflects the character of both the partially filled bands which give Fermi surface breaks, as well as the completely filled bands which yield more smooth variations in the momentum density. Recall that the Fermi surface of $YBa_2Cu_3O_7$ is predicted by band theory to consist of four sheets, the 'electron ridge', the 'pillbox', and two closely placed 'barrels'. In Fig. 7 the signatures of the electron ridge Fermi surface are the break around $r_0$ in the first Brillouin zone (the break at the reflected point $-r_0$ not shown), its first 'umklapp' image ($r_1$,$r_2$) around 6.3 mrad, and the second image ($r_3$,$r_4$) around 12.6 mrad. The ridge Fermi surface arises from a highly anisotropic one-dimensional band which is essentially full along ΓX but nearly empty along the ΓY direction. The associated electronic states couple strongly with the positron state in $YBa_2Cu_3O_7$ and yield clear features of the sort seen in Fig. 7. We also see other Fermi surface features in Fig. 7; most notably the breaks denoted by ($s_1$, $s_2$, $s_3$, $s_4$) and the umklapp images ($s_5$,$s_6$) in the lowest panel, all arising from a small hole Fermi surface (the pillbox sheet) centered around the symmetry point S.

The theoretical and experimental anisotropies in the form of difference sections are compared directly in Fig. 8. We see that the theoretically predicted shapes are in remarkable accord with the experimental results with (right set) as well as without (left set) the background correction. The discrepancies of the level seen in Fig. 8 are common in first principles comparisons of this sort in even simpler transition and noble metals. By correcting for the background, the agreement is in fact improved, e.g., the dip in the theory ΓS-ΓY curve around 6 mrad is better reproduced in the corrected data. Most important, if the data is not corrected for the background, the absolute magnitude of the experimental anisotropy (dashed curves in the right set) is only about half as large as the theoretical predictions; this discrepancy is seen to be essentially removed by correcting for the background; a similar improvement in this regard was found in connection with Fig. 6 above for the original spectra.

We comment briefly on the comparison between theory and experiment with regard to Fermi surface signatures in the anisotropic spectra; this question is considered further by Bansil and Smedskjaer [18]. Most notably, the detailed signatures of the ridge Fermi surface are observed clearly in the data. These are: (i) The rapid decrease or increase in the various sections of Fig. 8 around zero momentum is consistent with the break $r_0$ (Fig. 7), although the experimental points suggest a larger width of the ridge than inherent in our band structure (see especially panel 3); this has also been noted by others [8]. (ii) The first umklapp image ($r_1$, $r_2$) of the ridge around 6.3 mrad predicted by the theory is seen at least as a shoulder in frame 3. (iii) The second image ($r_3$,$r_4$) of the ridge theoretically yields a feature after resolution broadening around 13 mrad ($r_4$), which is generally consistent with the data, and in particular with the zero crossing seen in the data in frame 2 around 13 mrad [24]. Interestingly, the dip in the theory in the XS-YS anisotropy between 9 and 10 mrad due to the pillbox Fermi surface

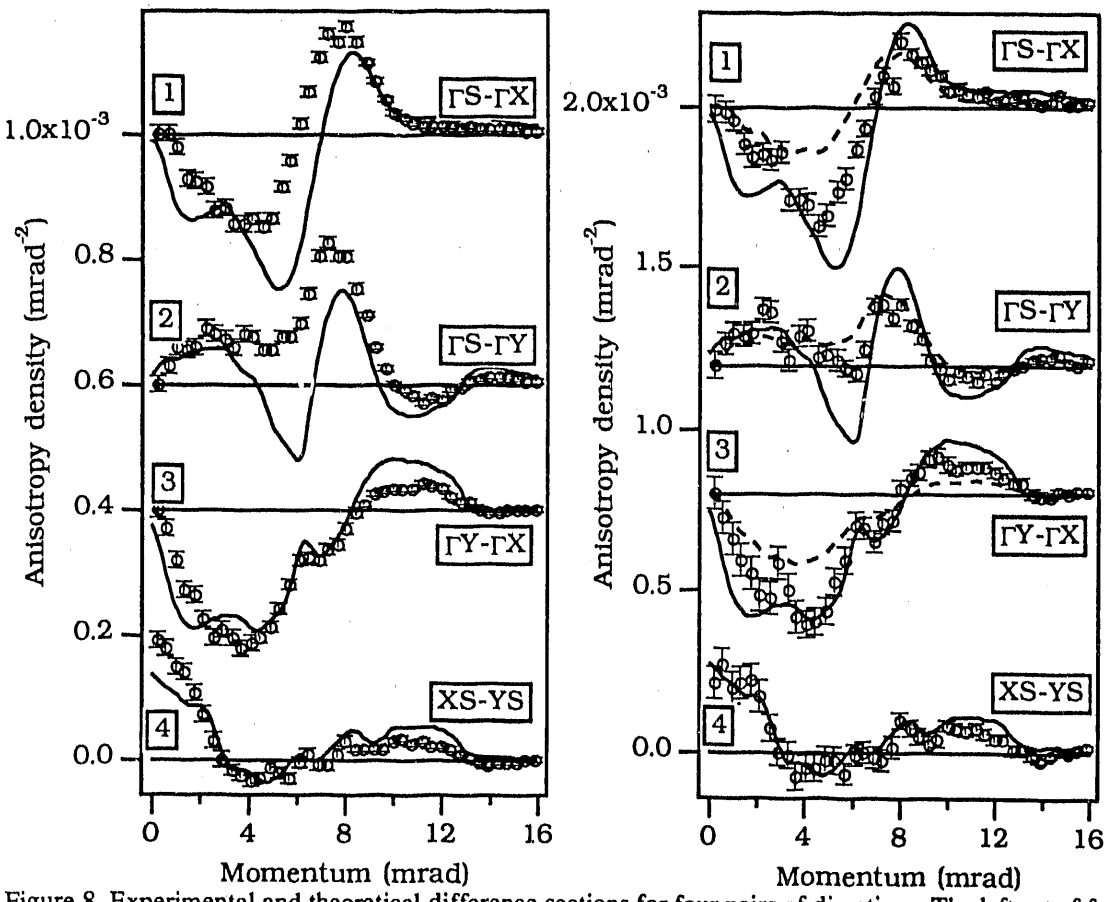


Figure 8. Experimental and theoretical difference sections for four pairs of directions. The left set of frames are obtained from the as observed 300K data, while the right set is based upon the 'background corrected' spectrum H(**p**) shown in Fig. 6. The theoretical results (solid curves) are obtained by resolution broadening (corresponding to 300K) of the data of Fig. 7; the difference between the left and right sets of the theoretical results is that in the left set the theory is arbitrarily normalized to produce a visual agreement with experimental results (using the same constant scale factor for all curves), whereas in the right set the comparison between the theory and experiment is on an absolute scale. For reference, the 300K experimental curves of left set are also shown by dashed lines on the right set of frames for an absolute comparison.

(Figs. 7 and 8), is rather well reproduced in the measurements; this point however needs to be analyzed further.

## CONCLUSIONS

In summary, we have carried out 2D-ACAR positron experiments on an untwinned single crystal of metallic $YBa_2Cu_3O_{7-x}$ as a function of temperature over the range 30K to 300K. We show that, to a good approximation, the temperature dependent data can be described as a superposition of two temperature independent spectra whose relative weights vary with temperature. On this basis, we suggest that the observed spectra may be viewed as resulting mainly from two mechanisms, namely, annihilations involving the positron in the Bloch-state, and other 'background' annihilations. The detailed nature of the 'background' annihilations is unclear, although the temperature dependence suggests that the process would involve one (or more) shallow traps. We discuss how the temperature dependent data can be used to extract a 'background corrected' spectrum; the resulting experimental spectrum is found to be in remarkable agreement with the corresponding band-theory based predictions, with regard to not only the shape and characteristic anisotropies, but also the absolute amplitude of the anisotropy. Furthermore, the observed spectra clearly display the distinct signatures of the electron ridge Fermi surface in accord with theoretical predictions. The presence of a signature of the pillbox Fermi surface is also indicated, although this point needs further study.

Work supported by the U.S. Department of Energy, Basic Energy Sciences, Division of Materials Sciences under contract #W-31-109-ENG-38 (LS), and under a subcontract to Northeastern University (AB). This work benefited from the allocation of supercomputer time on the NERSC and San Diego Supercomputer centers.

References

[1] Peter M., Hoffmann L., and Manuel A.A, Physica C, 1988, 153-155 1724
Hoffmann L., Manuel A.A., Peter M., Walker E., and Damento M.A. Europhys Lett.,1988, 6 61
Hoffmann L., Manuel A.A., Peter M., Walker E., and Damento M.A. Physica C.1988, 153-155 129
Peter M., IBM J. Res. Dev., 1988, 33 333
Peter M., Hoffmann L., and Manuel A.A.: in *Positron Annihilation* 1988, Edts: Dorikens -VanPraet L., Dorikens M., and Segers D. World-Scientific, Singapore p. 197.

[2] Smedskjaer L.C., Liu J.Z., Benedek R., Legnini D.G, Lam D.J., Stahulak M.D., Claus H. , and Bansil A., Physica C, 1988, 156 269

[3] Peter M., Manuel A. A.: Phys. Scr. 1989, T29, 106

[4] Haghighi H., Kaiser J. H., Rayner S., West R.N., Fluss M. J., Howell R. N., Turchi P. E. A., Wachs A. L., Jean Y. C., and Wang Z. Z.: J. Phys.: Condens. Matter 1990, 2, 1911

[5] Barbiellini B, Genoud P., Henry J.Y., Hoffmann L., Jarlborg T., Manuel A.A., Massida S., Peter M., Sadowski W., Scheel H.J., Shukla A., Singh A.K., and Walker E.: Phys Rev B, 1991, 43(10), 7810

[6] Haghighi H., Kaiser J.H., Rayner S., West R.N., Liu J.Z., Shelton R., Howell R.H., Solar F., and Fluss M.J.: Phys. Rev. Lett., 1991, 67, 382, and J. Phys. and Chem. of Solids, 1991, (to appear)

[7] Smedskjaer L.C., Bansil A., Welp U., Fang Y., and Baily K. G.: J. Phys. and Chem. of Solids, 1991, (to appear)

[8] Hoffmann L., Sadowski W., and Peter M.: this conference

[9] Berko S., and Plaskett J.S.: Phys. Rev. ,1958, 112, 1877

[10] Bansil A., Pankaluoto R., Rao R.S., Mijnarends P.E., Prasad R., and Smedskjaer L. C.: Phys. Rev. Lett.,1988, 61, 2480 .

[11] Bansil A., Mijnarends P.E., and Smedskjaer L.C.: Phys. Rev. B, 1991, 43(4), 3667

[12] Bansil A., Mijnarends P.E., and Smedskjaer L.C.: Physica C,1990, 172, 175

[13] Bansil A. : J. Phys. and Chem. of Solids, 1991, (to appear)

[14] Massida S.: Physica C,1990, 169,137

[15] Massida S, Yu J., Freeman A.J., Hoffmann L., Genoud P., and Manuel A.A.: J. Phys. Chem, 1991, (to appear).

[16] Singh D., Pickett W.E., von Stetten E.C., and Berko S.: Phys. Rev. B, 1990, 42, 2696

[17] Berko S., Singh D.J., and von Stetten E.C.: J. Phys. and Chem. of Solids, 1991, (to appear)

[18] Bansil A., Smedskjaer L.C.: This Conference

[19] Smedskjaer L.C., and Legnini D.G.: Nucl. Inst. Meth. Phys. Res.,1990, A292, 487

[20] Hoffmann L., Sadowski W., Shukla A., Adam Gh., Barbiellini B., and Peter M.: J. Phys. and Chem. of Solids, 1991, (to appear)

[21] Golub G.H., and Van Loan C.F. *Matrix Computations* 1983, Johns Hopkins University Press (Baltimore), Chapter 12.

[22] Smedskjaer L.C.: *Positron Solid-State Physics*, 1983, Proc. of Int. School of Phys. "Enrico Fermi", 597, Edts: W.Brandt and A. Dupasquier, North-Holland Publ. Comp..
Smedskjaer L.C., Manninen M., and Fluss M.J.: J. Phys. F., 1980, 10 2237

[23] Fluss M.J., Berko S., Chakraborty B., Hoffmann K.R., Lippel P., and Siegel R.W.: J. Phys. F: Met. Phys, 1984, 14 , 2831

[24] Concerning the sharpness of the second image of the ridge around 13 mrad (frame 3), we have compared theory (scaled to coincide with the data in this region) to the data. We find that the experimental data do possess an edge around 13 mrad, which is as sharp as predicted by the resolution broadened theory.

# END

# DATE FILMED

3/12/92